

African Research Review

An International Multi-Disciplinary Journal, Ethiopia

Vol. 3 (5), October, 2009

ISSN 1994-9057 (Print)

ISSN 2070-0083 (Online)

Numerical Implementation and Computer Simulation of Tracer Experiments in a Physical Aquifer Model

Ojuri, Oluwapelumi. O. -Department of Civil Engineering, Federal University of Technology, Akure, Ondo State, Nigeria
E-mail: ojurip@yahoo.com,

Ola, Samuel A. - Department of Civil Engineering, Federal University of Technology, Akure, Ondo State, Nigeria
E-mail: samuelola41@yahoo.com,

Abstract

The numerical model Sand Model was developed and used to replicate the laboratory sand tank model. The plots of the TBCs for the twelve (12) multi-level observation points within the model domain show a reasonable match of the simulated and observed tracer breakthrough curves. The calculated t value (Paired- t test statistic) for each well is less than the critical value of t ($t_{critical} = 2.16$ for $df=13$), and the calculated P value for each well is greater than the chosen significance level ($P=0.05$), therefore the null (no difference) between observed and simulated data sets hypothesis is accepted. The analysis also reveals high to very high correlation between the observed and simulated values (Average $R^2 = 0.86$). It took eight (8) and Twelve (12) hours respectively for the tracer to reach its peak concentrations of 3.81mS/cm and 1.55mS/cm respectively for the middle (observation point (B_M) [x,y,z] [70,15,24]) and down gradient observation point (E_M) [x,y,z] [30,15,24]) within the sand tank model. A sensitivity analysis showed that the time required for complete source depletion, was most dependent on the source definition and the hydraulic conductivity K of the porous medium. The 12000mg/l chloride tracer source was almost completely dispersed within 34 hours.

Keywords: Replication, Numerical simulation, Model validation, Solute transport parameters, Tropical soil

Introduction

Physical aquifer model (Figure 1) was numerically replicated for the simulation of ground water flow and contaminant transport in a tropical porous media soil. Groundwater simulation models are used to conceptualize flow and contaminant transport, enabling geoscientists and engineers to bridge the gaps in the typically undersampled subsurface environment (Juyoul et al., 2005). While the major flow and transport processes associated with such models are understood, the specific parameters describing a given system need to be determined by calibrating ground water models according to laboratory and field observations. A great deal of effort and resources are expended on subsurface sampling in support of parameter identification, and tools providing time/cost savings are always of the utmost interest in the field. This work describes and demonstrates the novel integration of laboratory physical aquifer model and a numerical model.

The objectives of this research were to complete an experimental investigation to study the movement and dispersion of an injected chloride trace source in a three-dimensional sand tank model and evaluate relevant solute transport parameters for the tropical porous media soil. The data collected from the experiments was used to develop and test a detailed numerical modeling framework for simulating solute transport processes in saturated ground water aquifers.

Background

Water flow and transport of solutes through soils or other porous media are largely influenced by the macro structure of the porous medium, as has been shown by numerous experimental and numerical investigations in recent years (e.g., Hancock et al., 2008; Hassan et al., 2008; Dong et al., 2009). Unraveling the relations between the structural and chemical properties of a soil and its flow and transport behavior is still one of the main research areas of geoenvironmental engineering. It seems to be commonly believed that flow and transport could be simulated successfully, if only the geotechnical and hydraulic properties of the soil were known in sufficient detail.

Several studies have examined contaminant transport and natural attenuation in porous media soils. Studies have examined data derived from laboratory experiments (Jebellie et al., 2004; Sanyal and Kulshrestha, 2003; Iversen et

al., 2008) and field sampling efforts (Ola and Ojuri, 2008; Wang et al., 2009). Results of these studies have shown that numerical modeling technique generally give useful information on the estimation of solute transport parameters for various soils and the simulation of contaminant fate and transport in porous media. Numerical models, including MT3DMS (Zheng and Wang 1999), RT3D (Clement et al, 2004), MODFLOW (Harbaugh and McDonald. 2004), BioRedox- MT3DMS (Carey et al., 1999), Bioplume III (Rifai et al., 1997), and Hydrogeosphere (Therrein et al., 2004), have been used in conjunction with field and laboratory data to examine the capabilities of models to simulate contaminant transport and to identify factors affecting attenuation.

Model Equations and Methods

Governing Equations

For a homogeneous anisotropic system with coordinate directions aligned with the principal directions of anisotropy, the governing equation for 3D ground water flow is:

$$K_x \frac{\partial^2 h}{\partial x^2} + K_y \frac{\partial^2 h}{\partial y^2} + K_z \frac{\partial^2 h}{\partial z^2} = S_s \frac{\partial h}{\partial t} \quad (2.1)$$

Where K= Hydraulic conductivity , S_s = Storativity, h = Hydraulic head

The advective-dispersive transport equation becomes, in summation form:

$$\frac{\partial}{\partial x_i} \left(D_{ij} \frac{\partial c}{\partial x_j} \right) - v_i \frac{\partial c}{\partial x_i} - R\lambda c = R \frac{\partial c}{\partial t} \quad (2.2)$$

$$R = 1 + \frac{\rho_b}{\theta} K_d \dots\dots\dots (2.2a)$$

$$\lambda = \frac{(\ln 2)}{t_{1/2}} \dots\dots\dots (2.2b)$$

Where c= concentration, t= time, v= velocity, x= distance along the direction of flow, D= dispersion coefficient, R= retardation factor, ρ_b = bulk density

(soil), θ = effective porosity (soil) K_d = distribution coefficient, λ = decay constant and $t_{1/2}$ = half-life. The dispersion coefficient is commonly assumed to be proportional to the flow velocity, i.e., $D = \alpha v$, where the proportionality constant α is termed dispersivity.

The partitioning between the solute mass and the sorbed mass is usually expressed by means of a functional relationship, which is a linear reversible partitioning process, under isothermal conditions, is expressed by:

$$s = K_d c \quad (\text{Freeze and Cherry, 1979}).$$

where K_d is the distribution coefficient.

Equation 3.2 can be written as:

$$\frac{\partial}{\partial x} \left(D_{xx} \frac{\partial c}{\partial x} \right) + \frac{\partial}{\partial y} \left(D_{yy} \frac{\partial c}{\partial y} \right) + \frac{\partial}{\partial z} \left(D_{zz} \frac{\partial c}{\partial z} \right) - v_x \frac{\partial c}{\partial x} - R \lambda c - R \frac{\partial c}{\partial t} = 0$$

or in vector form:

$$\text{div}(\mathbf{D} \nabla c - \mathbf{v} c) - R \lambda c = R \frac{\partial c}{\partial t} \quad (2.3)$$

The dispersion tensor \mathbf{D} has a similar form as the hydraulic conductivity tensor \mathbf{K} . The components of \mathbf{D} are defined, according to classical theory (Bear, 1972) as;

$$D_{ij} = \alpha r |v| \delta_{ij} + (\alpha_L - \alpha_T) \frac{v_i v_j}{|v|} + D^* \delta_{ij} \quad (2.4)$$

where α_L and α_T are the longitudinal and transverse dispersivities, respectively, and $D^* = D_d \tau$ is the effective diffusion coefficient in the porous medium, with D_d being the molecular diffusion coefficient in solution and τ the tortuosity of the medium, and δ_{ij} is the Kronecker delta.

For 1D transport, this equation simplifies to:

$$D = \alpha_L v + D^* \quad (2.5)$$

In two dimensions, the components of the dispersion tensor become

$$D_{xx} = \alpha_L \frac{v_x^2}{|v|} + \alpha_T \frac{v_y^2}{|v|} + D^*$$

$$D_{xy} = (\alpha_L - \alpha_T) \frac{v_x v_y}{|v|}$$

$$D_{yy} = \alpha_T \frac{v_x^2}{|v|} + \alpha_L \frac{v_y^2}{|v|} + D^*$$

In a 2D coordinate system following the principal directions of the dispersion tensor, which are parallel and perpendicular to the flow lines, these components simplify to:

$$D = \alpha_L v + D^*$$

$$D_{yy} = \alpha_T v + D^*$$

$$D_{xy} = D_{xx} = D_{yz} = 0$$

In 3D systems, there will be one direction of longitudinal dispersion and two directions of transverse dispersion. The classical dispersion theory holds only if the dispersivities in the two transverse directions are the same dispersion in the vertical direction in an aquifer is generally much smaller than transverse dispersion in the horizontal.

For $R=1$ and $\lambda=0$ (Advection-Dispersion Model / Non reactive Transport Model)

$$\frac{\partial}{\partial x} \left(D_{xx} \frac{\partial c}{\partial x} \right) + \frac{\partial}{\partial y} \left(D_{yy} \frac{\partial c}{\partial y} \right) + \frac{\partial}{\partial z} \left(D_{zz} \frac{\partial c}{\partial z} \right) - v_x \frac{\partial c}{\partial x} - \frac{\partial c}{\partial t} = 0 \dots(2.6)$$

Boundary and Initial Conditions

For modelling purposes, the sand tank model was conceptualized as a shallow unconfined aquifer comprised of gravelly sand as porous media material. The specified constant hydraulic heads at the up gradient and down gradient boundaries of the porous medium were 73cm and 68.5cm respectively. Type 2, zero-concentration gradient (Neuman) and Type 3, dispersive flux boundary (Cauchy) contaminant transport boundary

conditions were used. Instantaneous contaminant injection was used at an injection rate of 0.7ml/sec for 5 minutes. Background tracer concentration (c_0) was 0.288mS/cm.

Tracer was injected along the length of the source location (x,y) (110,15). The injection concentration of the tracer was 28.1mS/cm (12g/l) in line with the injection concentration for the physical aquifer model in the laboratory.

Modelling Techniques and Numerical Implementation

Solute transport parameters such as, dispersivity, dispersion coefficients, seepage velocity and effective porosity values of the sand tank were obtained from a tracer transport experiment.

The cell-centered finite difference equation was generated for the 3-D flow equation. The 3-D difference equation is:

$$K_x \frac{(u_{i-1,j,k} - 2u_{i,j,k} + u_{i+1,j,k})t}{\Delta x^2} + K_y \frac{(u_{i,j-1,k} - 2u_{i,j,k} + u_{i,j+1,k})t}{\Delta y^2} + K_z \frac{(u_{i,j,k-1} - 2u_{i,j,k} + u_{i,j,k+1})t}{\Delta z^2} = S_s \frac{(u_{i,j,k})t - (u_{i,j,k})t - \Delta t}{\Delta t} \quad (2.7)$$

Cell-centered finite difference equivalents for the 3-D Advection-Dispersion equation in equation 3.3 are given as;

$$D_x \frac{(c_{i-1,j,k} - 2c_{i,j,k} + c_{i+1,j,k})t}{\Delta x^2} + D_y \frac{(c_{i,j-1,k} - 2c_{i,j,k} + c_{i,j+1,k})t}{\Delta y^2} + D_z \frac{(c_{i,j,k-1} - 2c_{i,j,k} + c_{i,j,k+1})t}{\Delta z^2} = v \frac{(c_{i,j,k})t - (c_{i,j,k})t - \Delta t}{\Delta x} + \frac{(c_{i,j,k})t - (c_{i,j,k})t - \Delta t}{\Delta y} \quad (2.8)$$

We can again write the nodal template form by inspection directly from the difference equation. Multiplying the difference equation through by the volume $\Delta x \Delta y \Delta z$, and letting

$$a = \frac{D_{xx} \Delta y}{\Delta x}; \quad b = \frac{D_{yy} \Delta x}{\Delta y}; \quad c = \frac{D_{zz} \Delta x \Delta y}{\Delta z}; \quad V = v \Delta x \Delta y \Delta z$$

and $d = 2(a + b + c)$, the finite difference template becomes

$$\left\{ \underbrace{[-a \quad -b \quad -c \quad d \quad -c \quad -b \quad -a]}_M + \frac{1}{\Delta x} V \underbrace{[0 \quad 0 \quad 0 \quad 1 \quad 0 \quad 0 \quad 0]}_M - \frac{1}{\Delta t} \Delta x \Delta y \Delta z \underbrace{[0 \quad 0 \quad 0 \quad 1 \quad 0 \quad 0 \quad 0]}_M \right\} \begin{matrix} c_{i-1,j,k} \\ c_{i,j-1,k} \\ c_{i,j,k-1} \\ c_{i,j,k} \\ c_{i,j,k+1} \\ c_{i,j+1,k} \\ c_{i+1,j,k} \end{matrix}_t$$

$$= \frac{1}{\Delta x} V (c_{i,j,k})_{t-\Delta t} + \frac{1}{\Delta t} \Delta x \Delta y \Delta z (c_{i,j,k})_{t-\Delta t} \quad (2.9)$$

The global matrix equation will become;

$$\{ [M^D] + [M^V] + \frac{1}{\Delta t} [M^S] \} \begin{matrix} c_{i-1,j,k} \\ c_{i,j-1,k} \\ c_{i,j,k-1} \\ c_{i,j,k} \\ c_{i,j,k+1} \\ c_{i,j+1,k} \\ c_{i+1,j,k} \end{matrix} = \frac{\Delta x \Delta y \Delta z}{\Delta t} (c_{i,j,k})_{t-\Delta t} \quad (2.10)$$

Where the individual finite difference matrix templates are:

Dispersion matrix

$$[M^D] = [(-a)(-b)(-c).2(a + b + c)(-c)(-b).(-a)] \quad (2.11)$$

where

$$a = \frac{D_{xx} \Delta y}{\Delta x}; \quad b = \frac{D_{yy} \Delta x}{\Delta y}; \quad c = \frac{D_{zz} \Delta x \Delta y}{\Delta z};$$

Advection matrix (upstream-weighted form)

$$[M^V] = v_x \Delta y [-1..0..0..1..0..0..0] \quad (2.12)$$

Storage matrix

$$[M^S] = \Delta x \Delta y \Delta z [0..0..0..1..0..0..0]$$

This numerical technique entails using an upstream-weighted finite difference scheme for the advection term and an explicit scheme for the dispersion term in the ADE because these schemes were more stable. The method of finite difference was used to solve the 3-D groundwater flow and the Advection-Dispersion equation, while the FORTRAN 95 computer language was used to code the algorithm and develop the *SandModel* computer code. The results were displayed graphically using the MATLAB application package.

Input parameters used for the '*SandModel*' are based on the calibration of ground water flow and contaminant transport for the physical sand tank model and a review of the pertinent literature.

The experimental aquifer was discretized into 336,000 elements, comprising; 80 layers, 140 rows, and 30 columns ($n_i=140$, $n_j=30$, and $n_k=80$) (Figure 2). Details of the co-ordinates for the twelve observation points are in Table 2.1. Each grid cell was 1.0cm long by 1.0cm wide. The accuracy of a numerical model is partially governed by the grid spacing and time step constraints.

The grid spacing satisfies the grid Peclet constraints; $P_x = \frac{v_x \Delta x}{D_{xx}} \leq 2$

In the temporal domain, the time step satisfied the Courant criteria given by

$$C_x = \frac{v_x \Delta t}{\Delta x} \leq 1$$

The work on numerical modeling reported here quantitatively explores those patterns and predictions of groundwater and contaminant movement through the sand tank model. The primary tasks involved in developing the groundwater flow and solute transport model are 1) identifying a suitable

computer code; 2) selecting the vertical and horizontal extent of the model domain; 3) constructing a finite difference grid for the model domain; 4) overlaying the hydrostratigraphy onto the finite difference grid; 5) assigning boundary conditions to simulate natural hydrogeologic features of the groundwater flow system (Water table, rivers, water divides etc); 6) specifying hydraulic conductivity and other relevant material properties for each stratigraphic unit or layer. The flow charts for the main computer program and the two subroutines; Advection and Dispersion are illustrated in Figure 3a and Figure 3b.

***SandModel* Computer Code**

The computer program package developed for the numerical simulation is *SandModel*. It is a groundwater flow and solute transport simulation package developed during this research. The computer was written in FORTRAN 95 and was compiled using the Compaq Visual Fortran Compiler. It will run without modification without modification on any Microsoft Windows based PC with sufficient RAM. *SandModel* is a three-dimensional numerical model describing fully-integrated subsurface flow and solute transport. *SandModel* is a unique and ideal tool to simulate the movement of water and solutes within the subsurface in a realistic, physically-based manner. The *SandModel* code was designed so that it can be extended to handle more complex field problems in an efficient and robust manner. It's finite difference numerical approximation technique, fully-coupled analysis and it has compatibility with advanced visualization package MATLAB. For each time step, the model solves subsurface flow and mass transport equations simultaneously. The model input parameters are presented in Table 3.1

Model Results and Analysis

Concentration Breakthrough Profiles

The numerical model was run in the tracer mode to simulate the observed tracer breakthrough results. Multiple simulations were completed by adjusting the values of the longitudinal and transverse dispersion coefficients, and the value of the effective porosity to fit the breakthrough data collected at all the twelve observation points. A comparison of the measured and simulated breakthrough profiles are shown in Figure 4. Statistical comparison of observed and simulated data using the coefficient of determination (R^2), as correlation index and the Paired-t test of significance between sample means at 5% level of significance for the breakthrough

curves reveals a high correlation and that there is no significant difference between the observed and simulated data sets. The summary of the statistical analysis for the four observation wells are as follows;

Observation well B [$R^2=0.79$, $N=14$, Calculated $t=-0.579$ with df 13, $P=0.572$ (2-tailed)]

Observation well C [$R^2=0.91$, $N=14$, Calculated $t=0.540$ with df 13, $P=0.598$ (2-tailed)]

Observation well D [$R^2=0.86$, $N=14$, Calculated $t=1.046$ with df 13, $P=0.315$ (2-tailed)]

Observation well E [$R^2=0.88$, $N=14$, Calculated $t=1.98$ with df 13, $P=0.204$ (2-tailed)]

where; R^2 – Coefficient of Determination

N – Sample size

t - t-statistic(student t quantile)

df – degree of freedom ($N-1$)

P - calculated probability is the estimated probability of rejecting the null hypothesis (H_0) of a study question when that hypothesis is true.

Calculated t value for each well is less than the critical value of t ($t_{critical} = 2.16$ for $df=13$), and the calculated P value for each well is greater than the chosen significance level ($P=0.05$), therefore the null (no difference) between observed and simulated data sets hypothesis is accepted. The analysis also reveals high to very high correlation between the observed and simulated values.

Solute transport parameters can be determined by fitting the observed tracer breakthrough response to the Advection-Dispersion transport model for a conservative, nonsorbing solute in a homogeneous porous medium subject to unidirectional flow and three-dimensional dispersion (Kim and Harmon 2005). The calibrated estimates of the model parameter that best fit the profiles are the longitudinal dispersivity value of 0.07, transverse dispersivity value of 0.007, effective porosity value of 0.20 and seepage velocity of 2.2×10^{-5} m/s. These values are in good agreement with those obtained for a similar system (Dela Barre et al 2002, Juyoul et al., 2005).

Spatial Plume Description

The simulated spread of the injected tracer concentration in the XY-plane for 2, 4, 6, 8, 10, and 30 hours are shown in Figures 5 to 10. The view YZ and XZ planes in the sand tank for eight (8) hours simulation are presented in Figures 11 and 12. The isoconcentration contours in Figure 8, 11 and 12 confirms the peak observation of about 3.8 mS/cm concentration at point B_M (x,y,z) (70,15,24) for eight hours of simulation.

Sensitivity Analysis

One can analyze the effects of uncertainties associated with several of the modeled processes by studying the response of the calibrated model to systematic variations in the values of these model parameters. The uncertainty associated with the porous medium properties and bulk flow characteristics were analyzed by varying the hydraulic conductivity and dispersivity. The uncertainty associated with the source definition was analyzed by varying the source concentration.

In the first set of sensitivity simulations, a set of breakthrough profiles were generated using three orders of magnitude difference ($10K$ and $10^{-2}K$) from the measured value of hydraulic conductivity (K). Other model parameters were set at the base level used in the model calibration exercise. Figure 11 shows the sensitivity results for the breakthrough curves predicted at OW_{B_M}. The figure shows that one order of magnitude increase in the hydraulic conductivity value significantly reduces the concentration levels (42.3%). This is because, when the value of the hydraulic conductivity was increased, the size and connectivity of the porous media material pores increased; this in turn allowed easier flow of the contaminant and reduced residence time.

The second set of sensitivity simulations, studied the effects of variations in the source injection concentration. The injection concentration level is an important parameter that drives the spread of the contaminant. Under field conditions, the value of the source concentration can have considerable variations. In order to evaluate the variations in source concentration values, two additional simulations were completed using the concentration values 10,000 and 14,000mg/l. These two concentrations levels are arbitrary hypothetical values that were selected to assess the model sensitivity around the base case scenario. The results for these sensitivity simulations are summarized in Figure 12. The figure shows that the effects of variations in assumed concentration levels are more pronounced only during the initial stages of the tracer transport experiment. In addition as expected, the

predicted concentrations are high when the concentration level is high and they are low when the concentration value is low.

Conclusions

The developed computer application package *SandModel* was used to simulate the transport of an inorganic tracer (Chloride) in a laboratory aquifer model. The simulation results were visualized with the MATLAB application package. The modeling analysis identified two critical model parameters that include the porous media hydraulic conductivity, and the source concentration. Based on the model calibration results, the value of n_e was identified to be 0.20 for the experimental aquifer. This is about sixty three percent (63%) of the theoretical estimate. The sensitivity analysis showed that the time required for complete source depletion, was most dependent on the source definition, and the porous media hydraulic conductivity.

Acknowledgements

The authors would like to acknowledge the funding by the Federal University of Technology, Akure, Ondo State, Nigeria University Research Grant URG/MAJOR/2006/16, and the coding of numerical algorithm in FORTRAN by Babatunde J. Abiodun.

References

- Carey G.R., Geel P.J., and Murphy J.R. (1999) BIOREDOX-MT3DMS- A coupled biodegradation-Redox Model for simulating natural and enhanced bioremediation of organic pollutants. Conestoga-Rovers & Associates, 651 Colby Drive, Waterloo, Ontario, Canada, N2V 1C2
- Clement, P., Kim, Y., Gautam, R and Lee, K. (2004) Experimental and Numerical Investigation of DNAPL Dissolution Process in a Laboratory Aquifer Model. *Groundwater Monitoring & Remediation* 24(4):88 – 96
- Dong, D., Zhao, X., Hua, X., Liu, J., Gao, M. (2009) Investigation of the potential mobility of Pb, Cd and Cr(VI) from moderately contaminated farmland soil to groundwater in Northeast, China. *Journal of Hazardous Materials Elsevier* Volume 62, Issues 2-3, Pages 1261-1268[doi:10.1016/j.jhazmat.2008.06.032]

- Hancock T. C., M. W. Sandstrom, J. R. Vogel, R. M.T. Webb, E. R. Bayless, and J. E. Barbash (2008) Pesticide Fate and Transport throughout Unsaturated Zones in Five Agricultural Settings, USA *J. Environ. Qual.*, 37(3): 1086 - 1100.[doi: 10.2134/jeq2007.0024]
- Harbaugh, A.W., and M.G. McDonald. (2000). User's documentation for MODFLOW, an update to the U.S. Geological Survey modular finite-difference ground-water flow model. U.S. Geological Survey Open-File Report 96-485.
- Hassan G.,Reneau R.B., Hagedorn J.C., and Jantrania A.R. (2008) Modeling Effluent Distribution and Nitrate Transport through an On-Site Wastewater System. *J Environ Qual* 2008 37(5): 1937-1948. [doi:10.2134/jeq2007.0512]
- Iversen B.V., Van der Keur P., and Vosgerau H. (2008) Hydrogeological Relationships of Sandy Deposits: Modeling of Two-Dimensional Unsaturated Water and Pesticide Transport. *J Environ Qual.* 37(5): 1909-1917 [doi:10.2134/jeq2006.0200].
- Jebellie, S.J., A. Madani, and S.O. Prasher. (2004). Computer simulation of fate and transport of metolachlor in a soil column study. *Can. Water Res. J.* 29 :159–170.
- Kim J., Y. Park , and T.C. Harmon. (2005). Real-Time Parameter Estimation for Analyzing Transport in Porous Media. *Ground Water Monitoring & Remediation* 25, no. 2: pp78-86
- MATLAB v6.5. (2002). The MathWorks Inc. <http://www.mathworks.com/>
- Ola, S.A. and Ojuri, O.O. (2008): "Remediation of Hydrocarbon Contaminated Sites.", Paper presented at the 2ND ISSMGE International Lecture Tour in Environmental Geotechnics (NSE-NGA/ ISSMGE). , Lagos, Nigeria., 14-16, January.
- Therrien, R., Panday, S.M., McLaren, R.G., Sudicky, E.A., Demarco, D.T., Matanger, G.B., & Huyakorn, P.S. (2004) **HydroGeosphere** A Three-dimensional Numerical Model Describing Fully-integrated Subsurface and Surface Flow and Solute Transport, Waterloo Institute for Groundwater Research, University of Waterloo, Canada.

- Ursino, N., and T. Gimmi. (2004). Combined effect of heterogeneity, anisotropy and saturation on steady state flow and transport: Structure recognition and numerical simulation. *Water Resour. Res.* 40:W01514 [doi:10.1029/2003WR002180]
- Zheng C., and P.P. Wang (1999). MT3DMS: A modular three-dimensional multispecies model for simulation of advection, dispersion and chemical reactions of contaminants in groundwater systems- Documentation and user's guide. Contract report SERDP-99-1, U.S. Army Engineer Research and Development Center, Vicksburg, Mississippi.
- Wang, G., Lu, Y., Wang, T., Zhang, X., Han, J. Luo, W., Shi, Y., Li, J. and Jiao W. (2009) Factors Influencing the Spatial Distribution of Organochlorine Pesticides in Soils surrounding Chemical Industrial Parks. *J Environ Qual* 2009 38: 180-187.[DOI: 10.2134/jeq2008.0004]

Figure 1: Schematic Diagram of the Sand Tank Model

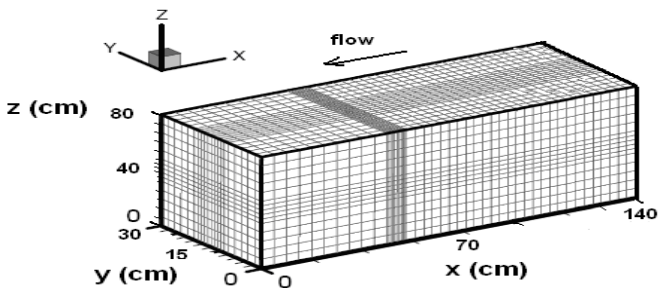
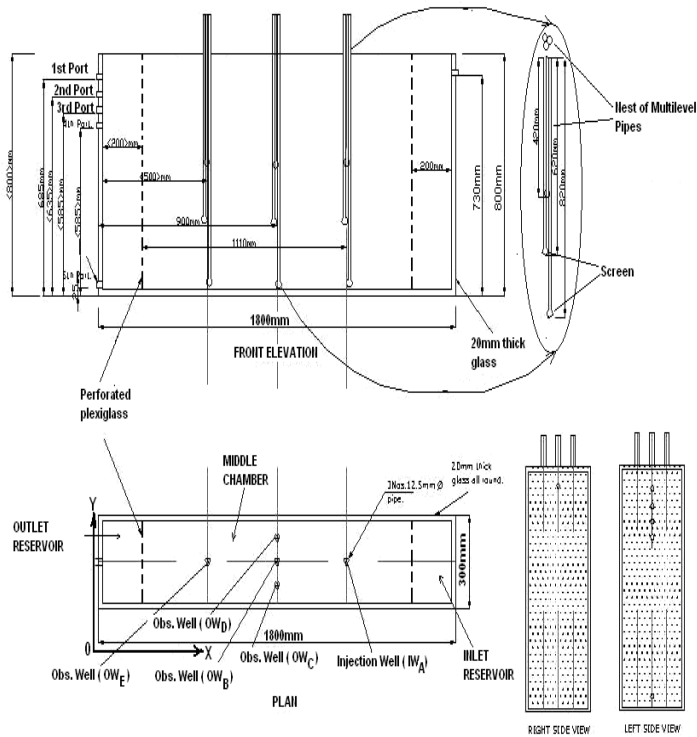


Figure2: Rectangular Finite Difference grids for the Sand Tank Model

Table 2.1: Co-ordinates for Observation Wells in the Sand Tank Model

BT (x,y,z)	BM (x,y,z)	BB (x,y,z)	CT (x,y,z)	CM (x,y,z)	CB (x,y,z)	DT (x,y,z)	DM (x,y,z)	DB (x,y,z)	ET (x,y,z)	EM (x,y,z)	EB (x,y,z)
(70,15,44)	(70,15,24)	(70,15,4)	(70,3,44)	(70,3,24)	(70,3,4)	(70,27,44)	(70,27,24)	(70,27,4)	(30,15,44)	(30,15,24)	(30,15,4)

MAIN PROGRAM

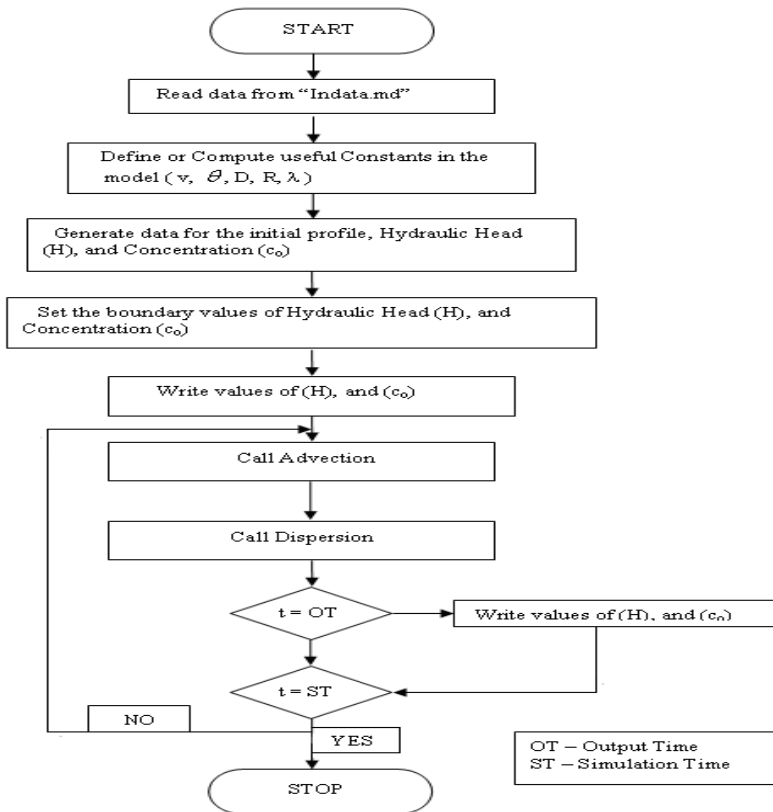
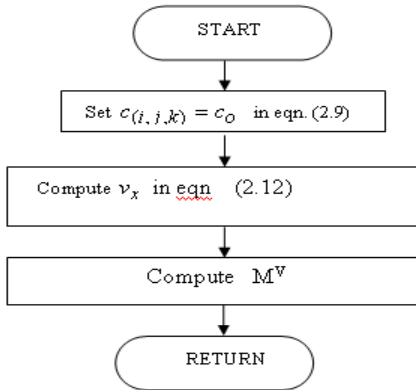


Figure 3a: Flow chart for Main Program

SUBROUTINE ADVECTION



SUBROUTINE DISPERSION

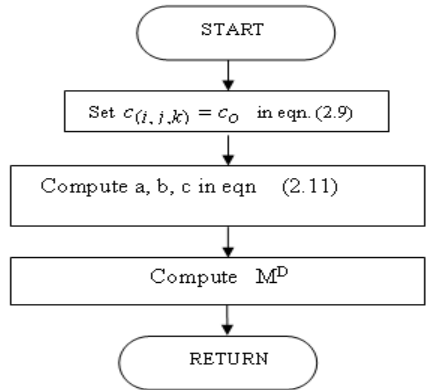


Figure 3b: Flow chart for Subroutines

Table 3.1: Flow system parameters used in simulating the laboratory scale tracer experiment

Parameter	Value	Source
dispersivity:		chloride tracer calibration
longitudinal (α_L)	0.06 cm	
transverse (α_T)	0.006cm	
Hydraulic conductivity (K_x)	5.76×10^{-4} m/s	measured
gradient	0.0321	measured
Porosity (n_e)	0.215	chloride tracer calibration
Velocity (v)	2.59×10^{-5} m/s	chloride tracer calibration
Bulk density (ρ_b)	1.9 Mg/m ³	measured
Median grain size (d_{50})	0.55	measured
Injection rate	12 ml/min	measured

Figure 4: Observed and Simulated Chloride Tracer Concentration Profiles for the Twelve (12) Multi-level Observation Points.

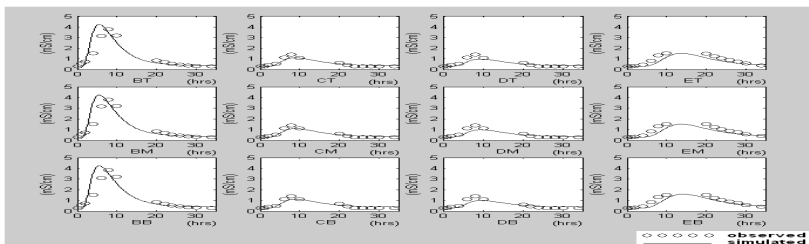


Figure 5: XY002 (Tracer Isoconcentration Contours after 2 hours)

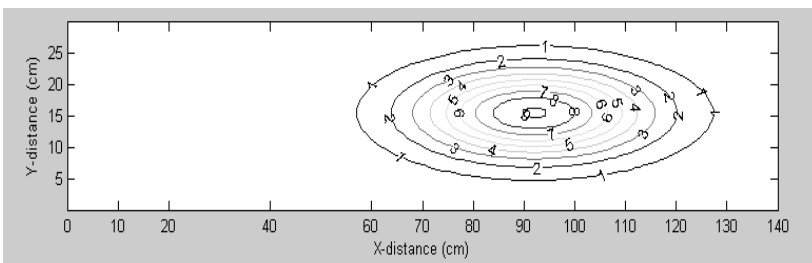


Figure 6: XY004 (Tracer Isoconcentration Contours after 4 hours)

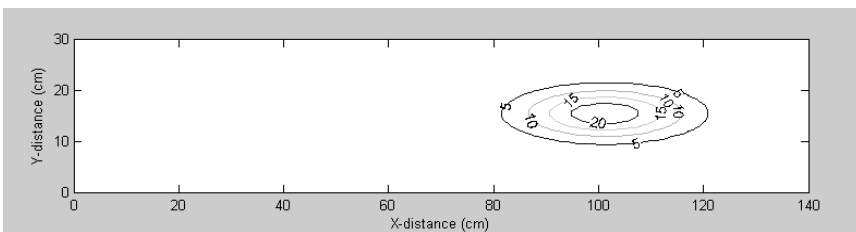


Figure 7: XY006 (Tracer Isoconcentration Contours after 6 hours)

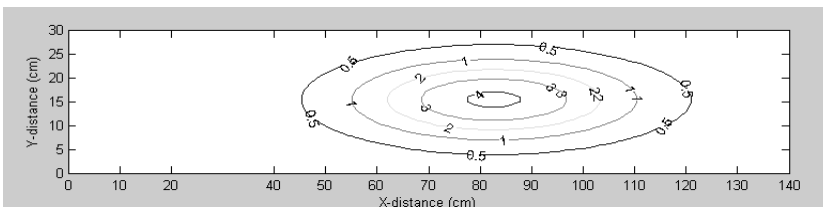


Figure 8: XY008 (Tracer Isoconcentration Contours after 8 hours)

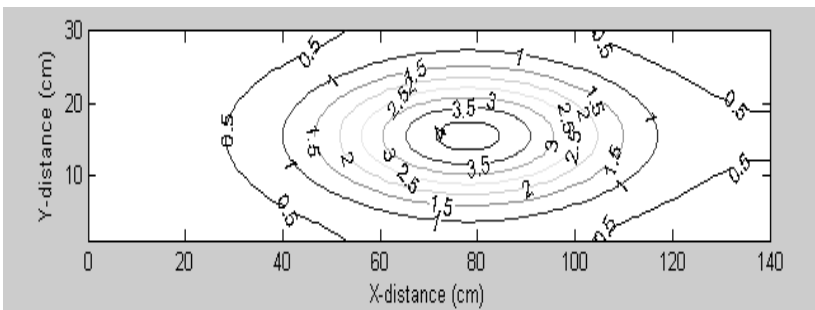


Figure 9: XY010 (Tracer Isoconcentration Contours after 10 hours)

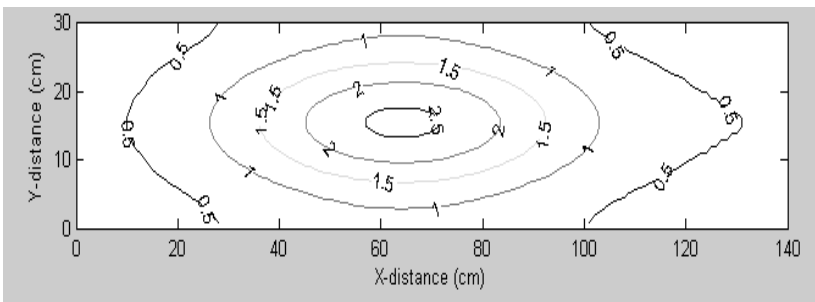


Figure 10: XY030 (Tracer Isoconcentration Contours after 30 hours

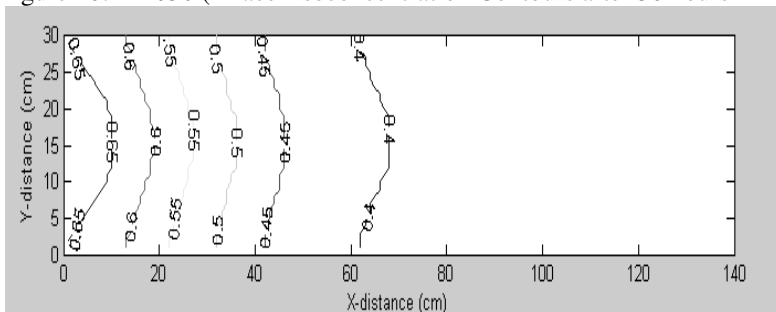


Figure 11: Tracer Plume at Observation Well B; Top, Middle, Bottom, 8 hours (YZ View)

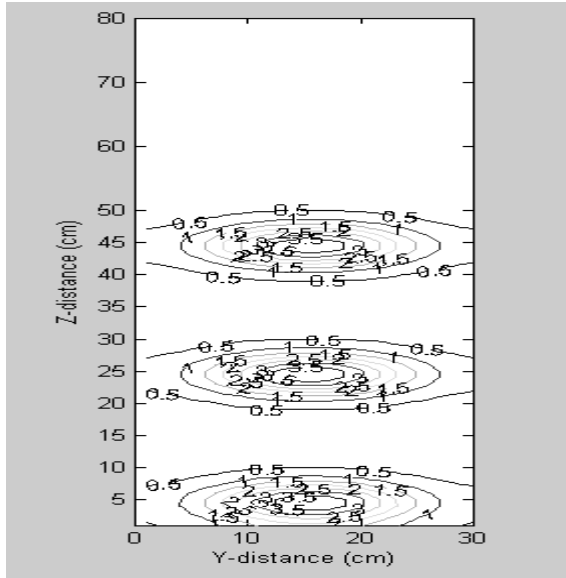


Figure 12: Tracer Plume at Observation Well B; Top, Middle, Bottom, 8 hours (XZ View)

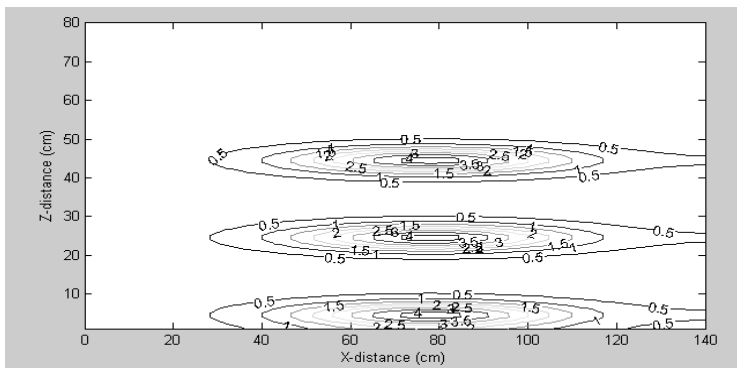


Table 4.1 Summary of Sensitivity

Variable	Value	Max. Plume concentration (mS/cm)	Δ Concentration with Respect to Base Case
Base Case		3.81	
Hydraulic Conductivity K	10K	2.18	- 42.3%
	0.01K	5.50	+ 44.4%
Dispersivity α_L	1000 α_L	3.20	- 16.01%
	1.0 α_L	3.81	0%
Source Concentration C	1.17C	4.78	+ 25.5%
	0.83C	3.24	- 15.0%

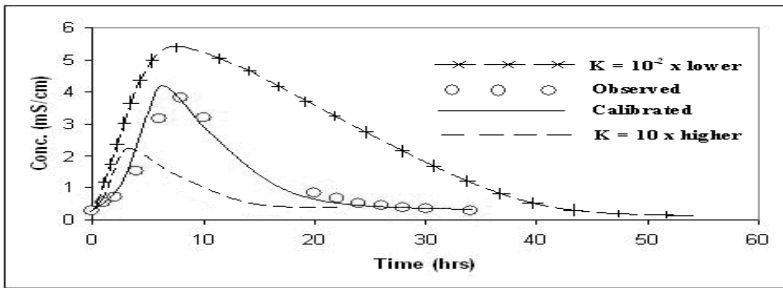


Figure 11: Model Sensitivity to Hydraulic Conductivity (Sampling location OW_{BM})

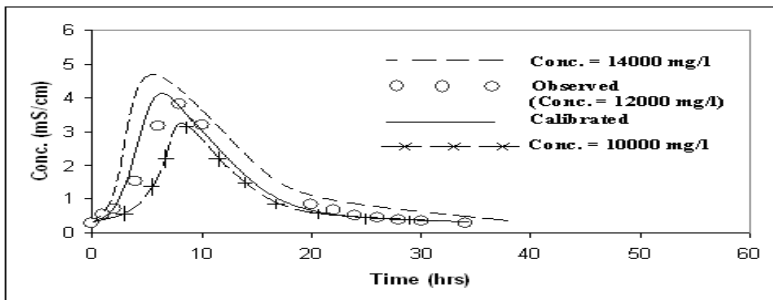


Figure 12: Model Sensitivity to Source Concentration (Sampling location OW_{BM})